Z-direction chemical analysis for new application methods

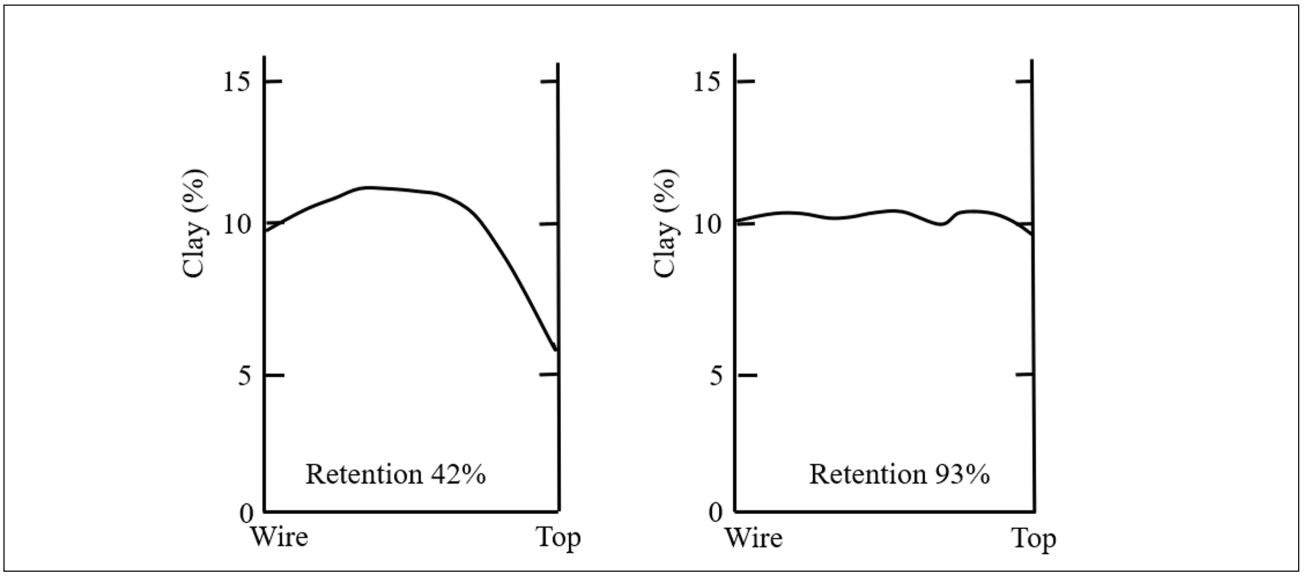
MATTHEW NICHOLAS, TERRY BLISS, AND TIFFANY BOHNSACK

ABSTRACT: In conventional wet-end chemical addition during paper production, chemical distribution through the z-direction of the sheet is usually not considered an important characteristic. With a nontraditional chemical dosing approach, such as foam-assisted additive addition, the chemistry can appear at different concentrations throughout the sheet, typically in a z-direction gradient. To fully understand the strength properties of the sheet, it is helpful to view or quantify the chemical distribution through the sheet in the z-direction. One qualitative method uses a dye technique along with confocal laser scanning microscopy to generate an image where the relative chemical concentration can be observed. A quantitative method involves compiling nitrogen analyses of layered subsections of the sheet into a composite graph of relative chemical concentration vs. the z-direction of the sheet. Chemical distribution analysis can be paired with traditional z-direction strength tests, such as Scott bond and z-direction tensile, to help one understand and improve the chemical addition process and its effects.

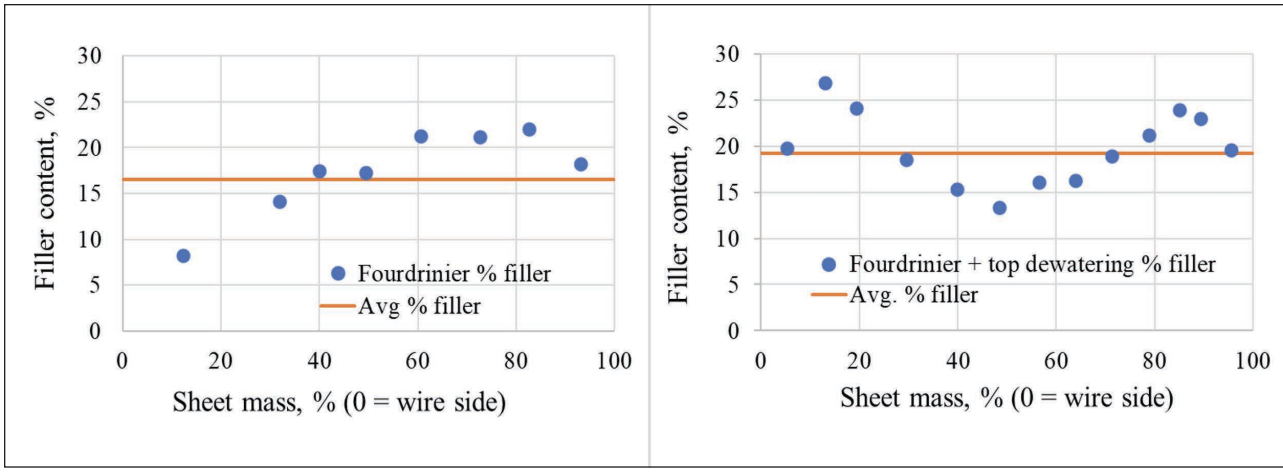
Application: This method can be used to determine the z-direction distribution of appropriate chemical additives in a sheet.

Paper is generally described as a 2-dimensional material, albeit with distinctly different properties in the machine direction (MD) than in the cross-machine direction (CD), and sometimes with distinctly different properties on the wire than on the felt side. The former is due to preferential fiber alignment and stretch in the MD during manufacturing, while the latter is due to the combined effects of filtration within the sheet in the z-direction and washout of fines and filler on the wire side. Handsheets typically form with little or no turbulence over the forming fabric, such that filtration is dominant; the lower half of the sheet (closest to the wire) is higher in filler and fines than the upper half (the felt side). The data in **Fig. 1** demonstrate how wire side filler content is higher when overall filler retention is low. When overall filler retention is high, the distribution is more uniform across the z-direction of the sheet [1].

By comparison, table activity in commercially formed paper has a much greater influence on the portion of the sheet closest to the forming fabric, such that washout of fine material tends to dominate, resulting in a very different z-direction ash and fines distribution. The degree of



1. Filler distribution in handsheets; the wire side filler content is higher than the felt side when the overall filler retention is low (left) but is more uniform when the overall filler retention is high (right). Redrawn from Tanaka et. al [1], Figure 1, Trials #9 and #11.



2. Filler distribution in uncoated freesheet varies by forming unit type: left, results from a 75 gsm sheet made with a fourdrinier former shows a single peak curve, with more filler near the top (felt side) and substantial turbulence-based depletion close to the wire; and right, results from an 80 g/m² sheet made with a fourdrinier with top dewatering unit shows a two-peak curve, with reduced filler in the center due to migration outward and turbulence-based depletion at the wire surfaces. The two-peak form is characteristic of all sheets with two-sided dewatering.

this impact is exaggerated when the overall retention is low.

The forming process (one-sided or two-sided dewatering) also influences the filler and fines distribution, with two-sided dewatering producing a sheet with two "wire" sides and a characteristic "M" shaped filler distribution, as shown in **Fig. 2**. We can assume that many other factors such as basis weight, fiber morphology, forming consistency, evenness of the water split, and turbulence levels in two-sided dewatering also influence these trends. In the case of multi-ply forming, each ply can be thought of as a separate sheet if the sheets are produced on mini-fourdriniers ("dry-on-dry forming") since the filler and fines cannot readily move between plies because of a lack of turbulence after the combining point. Multi-layer headboxes ("wet-on-wet forming") and secondary headboxes ("wet-on-dry forming") may be somewhere between single-sheet forming and dry-on-dry forming. The general trends for fines and filler distributions within sheets formed on a variety of single-ply former types are well documented [2].

Fines are chemically identical to fibers, but fines have a much higher specific surface area [3]. The mostly cationic wet-end additives tend to associate more with fines than fibers based on their surface area, especially if added in the thin stock circuit where the fines content is much higher because of the white water recirculation. This suggests that charged wet-end additives may display a non-uniform distribution in the z-direction because they preferentially associate with the fines; however, the impact of this association may be small, especially when the overall fines retention is high.

Not all additives are added in the wet end. Starch and other chemical additives can be added in the size press or as a coating. Many mills add starch or synthetic dry strength additives onto the forming section via a shower [4] or as a cascade [5,6]; interest in adding strength and other additives using foam application is growing [7,8]. When additives are applied as a foam on a sheet at 8%–10% consistency, little time exists for static attraction and little turbulence is available to influence fines washout. Additives vary widely by molecular weight, charge density, and the extent of their association with fibers or fines. We can expect some migration of additives within the sheet, but the extent of this migration has not been studied much to date.

The z-direction fines and filler distribution has been quantified by many techniques, including sheet splitting with adhesive tapes [1,9-12] or lamination devices [13], scanning electron microscopy/energy dispersive X-ray spectroscopy (SEM/EDX) scans of cut edges [14], differential freezing [15], sheet grinding [16], and in-plane microtoming [17]. Results from many other techniques are presented in the literature, but none are formalized as test methods at present. Most are used as in-house tests for a limited range of paper grades. Tape splitting is difficult for very thick and stiff paperboard sheets and does not always work well for coated grades, while SEM/EDX scans of very thin sheets are difficult to work with and low in accuracy for printing and writing grades, in our experience.

Most of these methods are not directly applicable for quantifying the distribution of chemical additives in the z-direction, except by a presumed preferential association of additives with fines. This association is probably not consistent enough to use effectively, but our expectation is that some of the identified trends would apply. A robust test for quantifying synthetic additives could be helpful for studying the z-directional distribution of additives, particularly for sprayed or foam-applied applications, where an additive distribution profile would be expected.

The z-direction distribution of starch has been reported, with examples from size press-treated and foam-applied starch highlighted [18]. This method involves cross cutting

the sheet, then spraying the cut edge with an iodine solution. The higher starch concentration areas appear as dark blue or brown and can be reported qualitatively or quantified by image analysis as depth of penetration or as a starch concentration distribution.

Dye may be added with functional additives applied via foam [6] and for sprayed additives or even size press and coater applied additives, at least in laboratory or pilot environments. However, because dye molecules may be much smaller than strength additives of interest and may have a different charge, this technique has some intrinsic limitations.

We are not aware of published efforts to quantify z-direction synthetic strength agent distribution. In this paper, we explored various methods of doing so. This is challenging because only 0.1%–0.4% dry solids of synthetic dry strength agents are added, compared to 1%–2% starch and up to 25% of inorganic fillers.

DEVELOPMENT OF METHODOLOGIES

We explored methods for adding products to a sheet beyond the traditional wet-end addition of chemicals. Recent development of the foam addition process [7,8] has highlighted the need for a method that can show the distribution of chemical additives in the z-direction of a final product.

Tape splitting followed by nitrogen content analysis

Several options were considered for determining the chemical distribution in the z-direction. Tape splitting followed by nitrogen content analysis was attempted first. The tape splits were successful; however, the nitrogen content of the tape's adhesive, while very low, was much higher than that of the additives, and its standard deviation was too high to reliably subtract out as a blank. We were reluctant to try removing the tape adhesive with solvent extraction, because it potentially could have also extracted some paper additives.

Fluorescent staining and confocal laser scanning microscopy

Fluorescent staining followed by confocal laser microscopy (CLSM) is a well-known method of visualizing chemical content, although not traditionally in the z-direction of the sheet. The fluorescent staining is not highly selective and can react with many materials, including other synthetic materials added in the wet end, such as a retention aid. Any amount of recycled material would also render the method less effective.

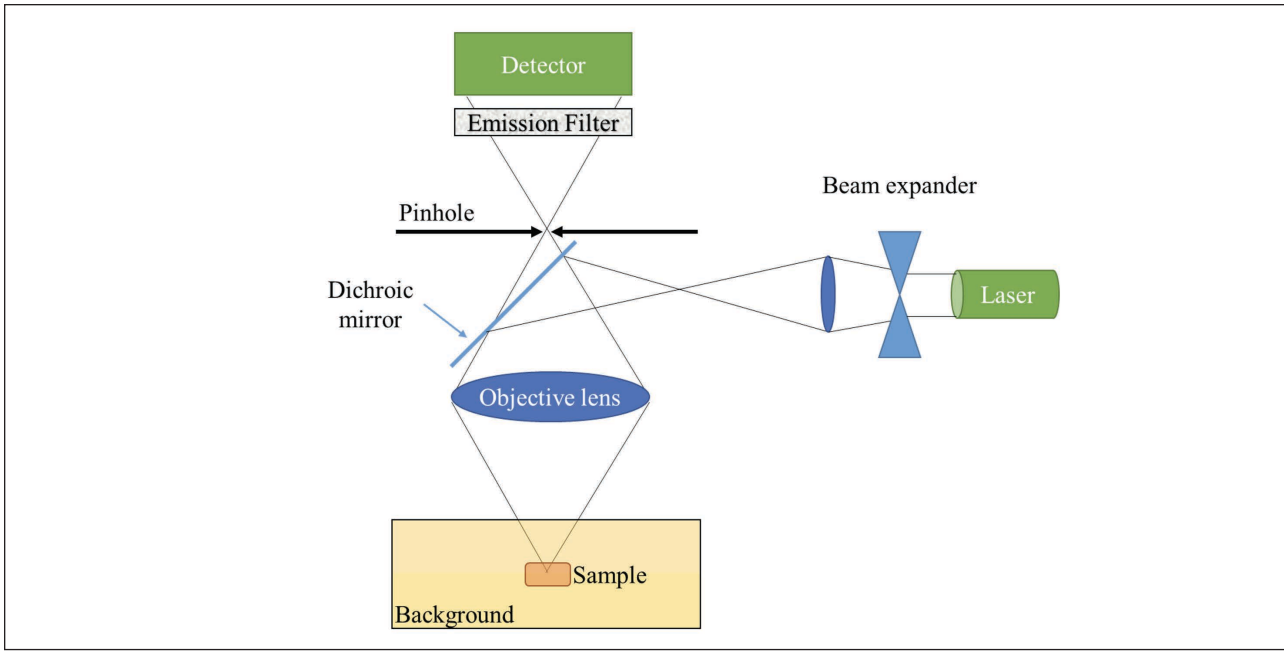
Sheet samples cut to 2.5 cm x 2.5 cm were stained with two fluorescent dyes. Sulforhodamine 101 (Sigma Aldrich; St. Louis, MO, USA) was used to stain the polyamide epichlorohydrin (PAE) resin, and acridine orange (Electron Microscopy Sciences; Hatfield, PA, USA) was used to stain the paper fibers. A self-bridge formation between the sulforhodamine 101 acid chloride anionic site and the PAE cationic site is expected to occur during staining [19]. Each paper section was soaked in a 0.005 wt% solution of sulforhodamine 101 for 3 min, rinsed (approximately 5 s) with distilled water, and then soaked in a 0.005 wt% solution of acridine orange for 3 min and rinsed (approximately 5 s) with distilled water. While acridine orange is not required to image the PAE, it helps to highlight the fibers' location and give good contrast in the processed images. Once staining was complete, the sample was dried at room temperature for a minimum of 24 h prior to imaging. If the z-direction cross-sectional analysis was required, the stained samples were mounted in TBS tissue freezing embedding medium (Triangle Biomedical Sciences (TBS); Durham, NC, USA), and sections were microtomed using a Leica 3050 cryostat (Leica; Wetzlar, Germany). Microtomed sections were collected and mounted on a microscope slide for CLSM imaging.

A Zeiss 880 confocal laser scanning microscope (Zeiss; Oberkochen, Germany) was used to study the location of the PAE resin in a paper sheet. Confocal laser microscopy is a non-destructive imaging technique that obtains an image by line-by-line scanning of the sample with a focused laser beam. A pinhole is used to block out-of-focus light, which increases the image resolution and contrast. A depiction of the laser path is shown in **Fig. 3**. Fluorescent staining was performed to determine the specific location of the PAE within the paper sheet. Multiple components can be imaged simultaneously by using fluorescent tags or fluorescent stains with different excitation and emission wavelengths. A 10x/0.45 (Zeiss Plan-Apochromat) dry objective lens was used for imaging. Laser lines at 561 nm (diode-pumped solid state [DPSS] laser) and at 458 nm (argon laser) were used because these wavelengths correspond with the emission wavelengths for sulforhodamine 101 and acridine orange. Z-stacks, which are a collection of optical sections that can be reconstructed as a 3D image, of each paper sheet were acquired. Images were processed in either the Zeiss Zen software or ImageJ software (National Institutes of Health; Bethesda, MD, USA).

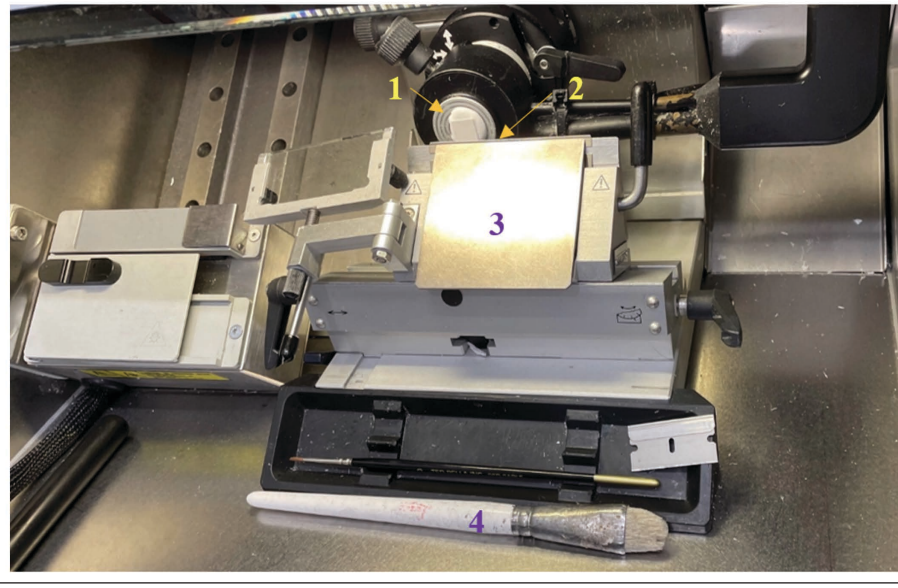
Layer sectioning and nitrogen analysis

A more quantitative method was desired. We considered the historic methods of differential freezing or sheet grinding (followed by nitrogen analysis), but the grinding or freezing equipment was not readily available. Therefore, we explored the microtoming equipment previously used for cutting perpendicular to the surface of the sheet for the fluorescent staining method. The same microtome was used to cut layers *parallel* to the surface of the sheet. The layers were collected and analyzed for nitrogen. The procedure details are discussed next. This method is quantitative and less subject to visual bias.

Samples were cut to approximately 0.75 cm x 0.75 cm. A sample holder was prepared by adding to it several drops of TBS tissue freezing medium and then placing it in a Leica CryoJane CM3050 S cryostat held at -25°C. A fresh dispos-



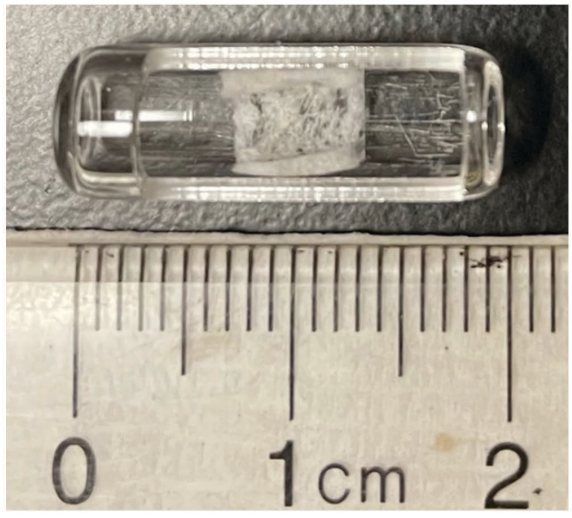
3. Example depiction of the laser path used in a confocal laser scanning microscope (CLSM) [20]. Mirrors initially tilt the laser beam in a raster mode in the x and y direction to the focus plane of the objective lens, which focuses the beam onto the sample. Once the laser beam reaches the sample, it is either transmitted through the sample, creating a transmitted image (not confocal), or the fluorescent (or reflective) light will pass back through the objective lens and the dichroic mirror then reflects the light back through the pinhole to the detector.



4. Image of the mounted sample just before initial slices. Location 1: white sheet sample mounted on Triangle Biomedical Sciences (TBS) tissue freezing medium (also white in frozen form). Grey sample holder is mounted in slicing position. Location 2: fresh steel blade to be used for slicing layers. Location 3: sample collection plate. Location 4: sample collection brush used to collect "crumbled" sections.

able steel blade with a polytetrafluoroethylene (PTFE) non-stick coating was used for each sample. The blade was manually adjusted to just touch the paper sample for the initial slice. The slicing depth was standardized at 40 µm. After a preparatory cut, slicing proceeded quickly through the depth of the sheet until the sample medium was reached, usually after 9–13 slices. Each sectioned sample was then analyzed for nitrogen content. The equipment is shown in **Fig. 4**.

Nitrogen analysis was conducted using the trademarked Antek MultiTek (Antek; North Arlington, NJ, USA). First, each layer weight was individually recorded to the nearest 0.001 mg. Each layer was then placed in a glass sample boat prior to loading and nitrogen analysis, as shown in **Fig. 5**.



5. Image of a sample layer in a crystal sample boat prior to being loaded.

The instrument destructively analyzes the sample for nitrogen via pyro-chemiluminescence, where the sample is oxidized at approximately 1000°C, forming nitric oxide (NO) from nitrogen-containing compounds. The NO is then reacted with ozone to produce nitrogen dioxide (NO_2) and light. The light is amplified and detected by a photomultiplier tube, and the light is then converted by the software to "nitrogen counts." These nitrogen counts directly correspond to the base level of nitrogen in the layer, plus any added nitrogen from the chemical addition process. Each layer's nitrogen count is divided by the mass to determine its nitrogen concentration. A diagram of the Antek MultiTek system is shown in **Fig. 6**. For each condition, three samples were sliced and tested separately, then averaged.

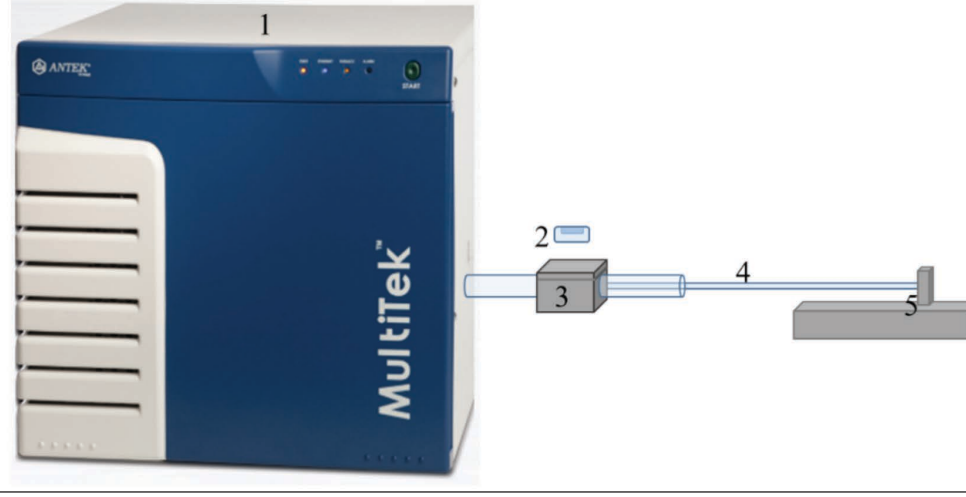
RESULTS

The preparation of sheets and the results for each method are discussed. The fluorescent staining and CLSM method results are qualitative images, while the layer sectioning and nitrogen analysis produces quantitative plots.

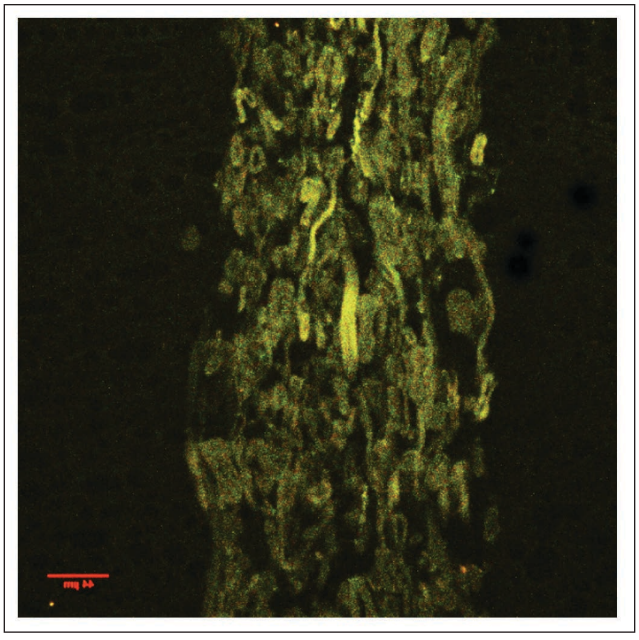
Fluorescent staining of paper samples and confocal laser scanning microscopy

The method was conducted on a set of handsheets prepared from bleached fibers of a 70% hardwood-to-30% softwood ratio. No additives were used beyond foam treatment of the handsheets immediately after formation and prior to vacuum, pressing, and drying. A blank handsheet with no foam treatment was prepared for comparison. The remaining two wet sheets were foam coated with a synthetic PAE resin at a dose of approximately 0.2% of final sheet mass. Foam at roughly 300 g/L density was applied to the surface of these wet handsheets in a 0.4 mm layer using our proprietary wet handsheet foam coating equipment and protocols, as described in the patent application [6]. One of these foam-treated sheets was air dried as a method check. All the PAE resin should be right at the top of this sheet after drying. The other wet sheet was foam coated in a similar way, and then vacuum was applied to pull the foam into the sheet and simulate the function of vacuum boxes on a paper machine. This sheet was then pressed and dried. All three sheets were then subjected to the fluorescent staining method, and the results are shown in **Figs. 7–9**.

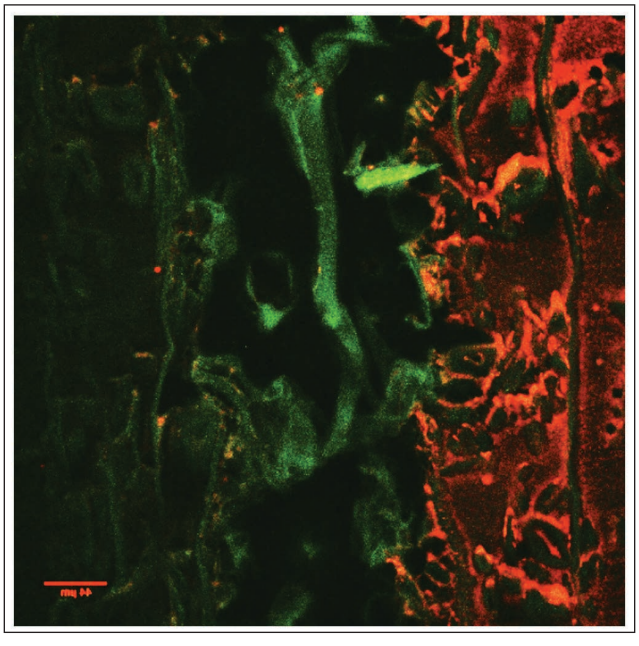
The fluorescent staining and CLSM method worked well for these handsheets produced without any wet-end additives. Although the images are qualitative only, they do show the first indication of the chemistry's location. However, there are some concerns with this method. Since the



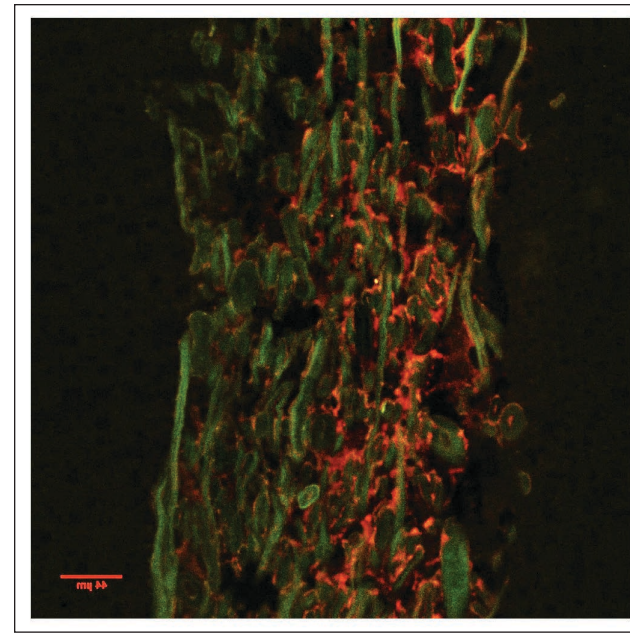
6. A diagram of the nitrogen analysis equipment. Location 1: the base unit. Location 2: a crystal sample boat, into which the sheet slices are individually loaded for analysis. Location 3: the sample loading box, which opens for placement of the sample boat into the equipment. Location 4: the loading arm, which holds the sample boat in an integrated tray at the end (located inside the loading box). Location 5: a mechanism that pushes the loading arm forward and into the base unit.



7. A processed scan of the untreated handsheet cross section, with the top of the sheet being on the right side of the image. The polyamide epichlorohydrin (PAE) shows as red, and fibers show as green. No red is visible, indicating that the sulforhodamine 101 intended to stain the PAE has good specificity and does not stain the fibers used for these handsheets. Therefore, this staining/microscopy method will work well for this sample.



8. A processed scan of the foam-coated, air-dried handsheet cross section, with the top of the sheet being on the right side of the image. The PAE mostly remained at the top of the sheet.



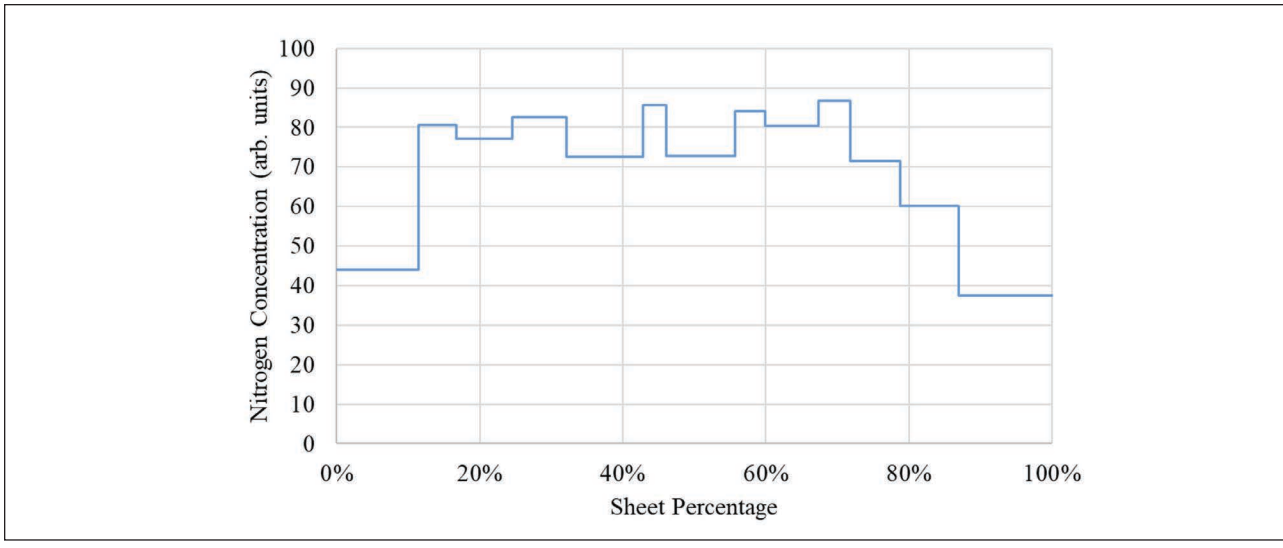
9. A processed scan of the foam-coated, pressed, and dried handsheet cross section, with the top of the sheet being on the right side of the image. The PAE shows as red, and fibers show as green. The image shows PAE is present throughout the sample, although more highly concentrated in the top half of the handsheet.

sheet is rewetted during the application of the dye, it is not known if any added PAE has the potential for partial migration; that is, after the sheet is dried a second time after the dyes, the final chemical distribution may be altered from its initial state.

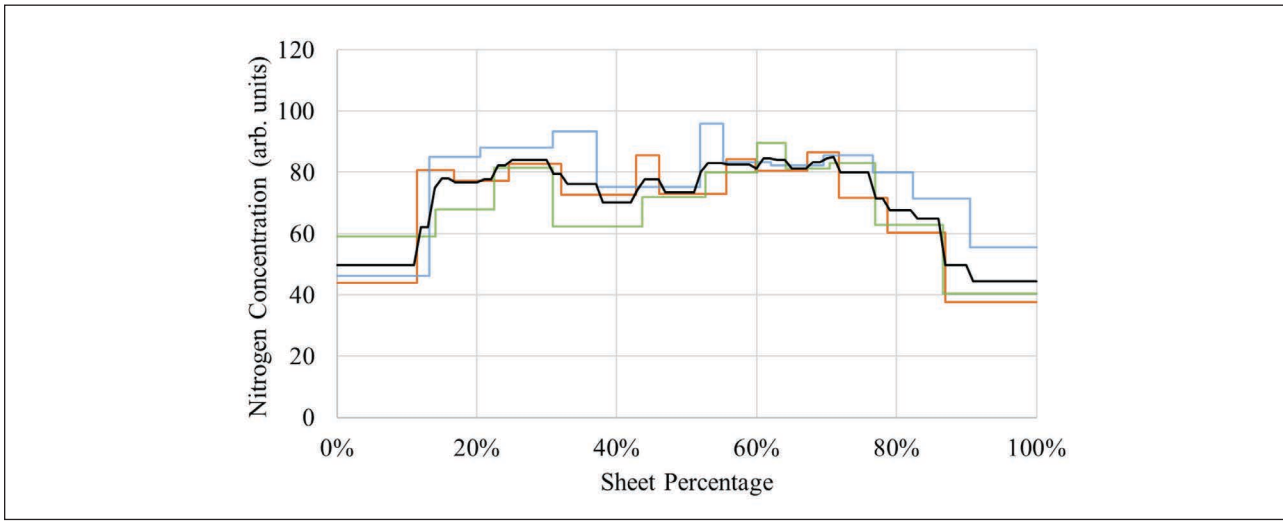
When applied to more realistic sheets that also contained commonly-used wet-end additives such as retention aids and cationic starch, we found these other additives also attracted the stain intended for the strength aid. This masked the distribution of the foam-applied chemistry, so the method failed. Some modifications, such as radioactive tagging or other modification to the PAE prior to foam application, were considered, but they were ultimately not investigated due to high cost and concern over potential impacts on the chemical distribution pattern. A method that tested finished sheets without rewetting and that used unmodified, commercially available materials was desired.

Layer sectioning and nitrogen analysis

The sheets prepared for this analysis were multi-ply (the plies had different furnish compositions) and were produced from a high-speed, realistic multi-layer papermaking trial. They underwent a similar foam application process: foam treatment after initial sheet formation, vacuum, and then pressing and drying. These sheets contained additives from traditional wet-end application, including retention aids and cationic starch. These materials prevented the CLSM method from being successful, so a layer sectioning and nitrogen analysis method was developed. The foam



10. A single sample's data from an untreated multi-ply sheet after the layering and nitrogen analysis was completed and the data was normalized. The nitrogen concentration is expressed in terms of nitrogen counts/mg and normalized by a factor of 2,000,000 to lower the scale. The sheet percentage indicates the depth into the sheet, with 0% being the bottom of the sheet and 100% being the top. The relative dry strength agent (DSA) concentration for each of 13 layers is distinctly visible.



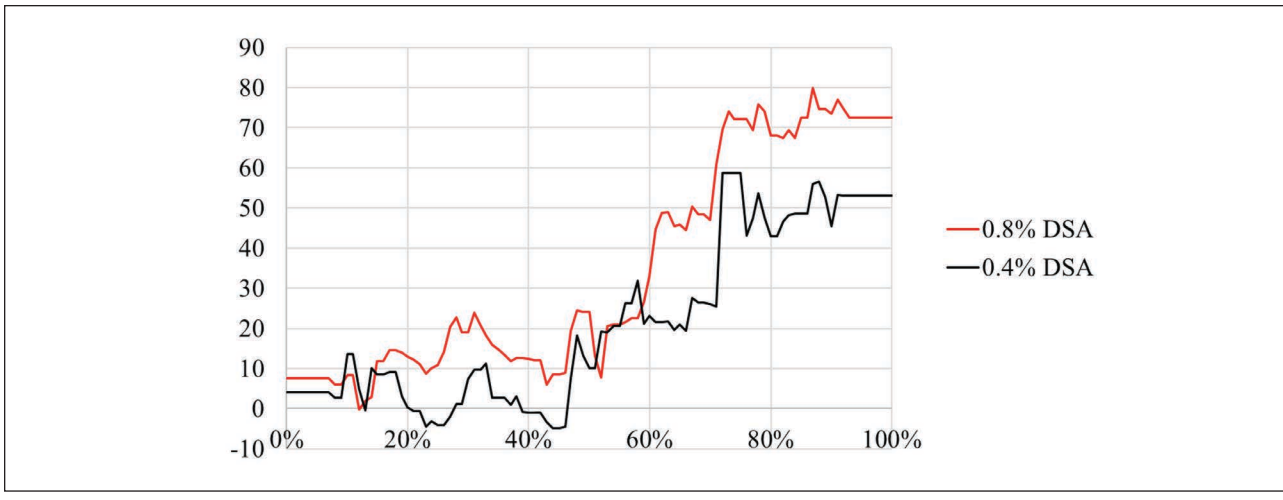
11. The composite of three samples for a single untreated multi-ply sheet is shown in black. Each individual sample's data from layer sectioning and nitrogen analysis is shown (orange, green, and blue lines). Variability was relatively low for this sheet, as is apparent from the small differences between the colored lines. The average value of the three individual samples is averaged together at each percentage point and plotted as the black composite line.

density was approximately 150 g/L and contained a foaming agent and a synthetic dry strength agent (DSA). The foam was applied between the first and second layers with the goal of providing local strength at and around the ply zone and increasing the strength of the second ply. An increase in z-direction strength performance indicated success and contributed to our understanding of how to control chemical penetration.

Multi-ply sheets with no foam treatment and additional sheets with foam-applied 0.4 w% and 0.8 w% DSA were prepared. The mass of each microtome layer was divided by the sum of all the layers, and the nitrogen data was presented as sheet mass percentage (0% is the sheet bottom and 100% is the top). The raw nitrogen counts of each layer are divided by the layer mass and a normalization factor of 2,000,000 to lower the scale. For example, a single untreated sample's plot is shown in **Fig. 10**.

Recognizing the potential sampling bias that a single preparation might incur, two additional samples for each condition were prepared in an identical manner, as previously described. Using the sheet percentages, the samples were averaged together at each point to provide a reasonable average composite for a single condition. This is shown in **Fig. 11**.

Next, the foam-treated multi-ply sheets were analyzed. The sample data for both foam-treated conditions, with



12. Distribution of added DSA within two foam-treated sheets: a 0.4%-dosed sheet and a 0.8%-dosed sheet. Concentration of the chemistry is shown to be lower for the 0.4% condition, as expected, but the two conditions follow similar chemical distribution patterns. Since the top ply accounts for approximately 23% of the sheet, the foam was added at 77% of the way through the sheet. The DSA concentration is highest at and around this point for both conditions, as expected. Based on the chemical distribution pattern, we consider it likely that any foam-applied chemistry that was not retained passed through the top layer of the sheet, likely during the pressing stage.

0.4w% and 0.8w% added DSA, were treated identically. The results in **Fig. 12** are shown with the average background nitrogen counts—in other words, the data shown in Fig. 11—subtracted from the foam-treated results. This data treatment removes the background nitrogen counts and provides a plot that represents the foam-applied DSA's distribution within the sheet. Some "negative" concentrations are observed, which indicate that the nitrogen concentration in the treated sheet was just below that of the blank at that location. This is to be expected with natural variations; realistically, this can be interpreted to mean a negligible amount of DSA was present at that location in the sheet.

DISCUSSION

The fluorescent staining and CLSM analysis method was the first successful attempt at imaging the distribution of foam-applied chemistry in the z-direction of the sheet. However, it was successful only in laboratory-produced handsheets with no other added chemistry. Attempts to analyze sheets with wet-end additives, as is ubiquitous in the industry, failed because of a strong stain response at all points in the sheet. Thus, it was not possible to separate the foam-applied additives from the background. This method is also primarily visual and not quantitative.

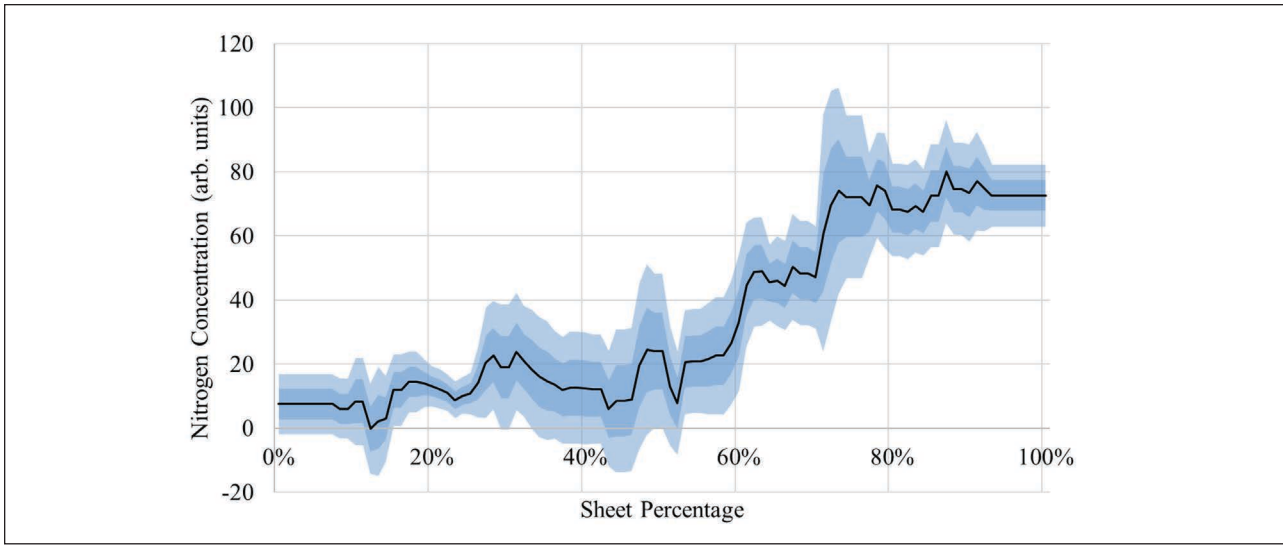
The cryostat layer sectioning and nitrogen analysis method is much more robust and quantifies the chemical distribution. By subtracting the nitrogen content of the background sheet, it is possible to view a foam-treated sheet's DSA distribution. Analysis of the chemical distribution can be paired with strength tests. For example, the location at which a sheet splits during z-direction strength testing (e.g., z-direction tensile [ZDT] or Scott bond) can be compared with the chemical distribution results. This may help determine the needed DSA dose and foam application parameters required to attain a target.

In Fig. 12, the chemical distribution of two sheets with different doses of a foam-applied DSA are compared. The chemical distribution is similar between the two, showing that most of the applied chemistry penetrates only to approximately halfway through the finished sheet, with the highest concentration in both cases around the application point between the two plies (77% through the sheet). Interestingly, the chemistry not only moved down into the sheet (the direction of the vacuum) but also migrated to the top 23% of the sheet; the top ply contains a high concentration of chemistry.

A ratio of the total applied chemistry between the two conditions can be approximated by integrating under the curve and comparing the total area for each condition. If the retention were identical, then exactly half the area would be expected for the 0.4% DSA condition vs. the 0.8%

Value	0.8% DSA Condition	0.4% DSA Condition
Area under the curve, Fig. 12	3462	2144
Retention	68%	79%
Expected area	-	2025

I. Area under the curve for both conditions in Fig. 12 and the conditions' separately analyzed retention results. An "expected area" is shown for the 0.4% DSA condition by dividing the 0.8% DSA area in half, then multiplying by a ratio of the two retention values. The expected area differs from the actual value by only 5.5%, providing some outside validation of the results.



13. A confidence interval plot for the 0.8% DSA condition when using this method. Nine samples were used to generate this plot, three times the typical number, and standard deviation was calculated at each point along the line using the 84 possible combinations of any three samples. The black line represents the average of all nine points. The dark blue area shows a single standard deviation from the mean, and the lighter blue area shows two standard deviations from the mean, for the average of three determinations.

DSA condition. However, separate analysis indicated retention of 68% for the 0.8% DSA condition and 79% for the 0.4% DSA condition. Higher retention is expected for lower dosage rates, as is commonly seen in the industry. Integration results and retention values are shown in **Table I**.

Initial conclusions made by direct observation of Figure 12 were that the pattern of chemical distribution was similar between the two and that the 0.4% DSA condition likely yielded higher retention, since its value does not appear to be half that of the higher dosage condition along the length of the curve. As shown in Table I, the integration of the plots matches reasonably well with separate retention analyses. This confirms the second conclusion and provides some support for the first; if the patterns were wildly different than pictured, the retention analysis would most likely not corroborate the integration.

Nine samples from a single sheet with 0.8% DSA applied via foam were tested for nitrogen counts, rather than the typical three samples, to investigate method reproducibility. By grouping these nine samples into all possible combinations of three, 84 possible combinations can be produced (${}_9C_3 = 84$). Averaging each of these groups of three together, as done for Figs. 11 and 12, yields 84 potential plots of chemical distribution for the same condition, allowing for reasonable standard deviation calculations. The standard deviation at each point in the sheet was calculated from these 84 averages of three determinations. The average outcome, obtained by averaging all nine samples, is shown as a black line in **Fig. 13**. A single standard deviation of the 84 averages of three results from the mean is shown as the darker blue shaded area, and the lighter blue shaded area captures two standard deviations from the mean. While there is visible variation, the pattern is mostly unchanged and would not impact the conclusions. Therefore, it is shown that this method can consistently produce a similar pattern. The data from this exercise could be used to determine how many samples must be processed to produce a result that is within a targeted accuracy. We believe that an average of three is sufficient for most applications.

Even though the layer sectioning and nitrogen analysis method appears to be robust, it does have limitations. The thickness of the sheet must be substantially larger than the practical layer thickness. The layer depth we used was 40 µm; therefore, analysis of a sheet with a thickness of 80 µm or less would yield little useful data. There is most likely an impact from the tissue freezing medium used during the cryostat sectioning. Although the freezing medium was verified to have negligible nitrogen concentration, the sample is placed directly onto the medium; thus, it is almost certain that the last slice will contain at least some of this material. The data is presented as a concentration of nitrogen counts/mg, so the additional mass very likely depresses the response of this top slice (roughly 90%–100% in the plots). However, this impact is minimized by subtraction of the background correction of the final chemical distribution results, because the effect will be present in both the untreated and treated sheets. Lastly, if the sheet does not have sufficient internal bond strength, the knife can crumble the sheet rather than cleanly slicing the sample. If the sheet crumbles, some material may be lost prior to collection and nitrogen analysis, and the sections will not be as clearly defined. These variables must be assessed for each new material tested with this method to ensure the method parameters are appropriate.

We continue to monitor and improve this method. For example, it quickly became apparent that the directionality

of the slicing method—whether top-down or bottom-up—would influence the results. Sheet slices were more uniform and intact when the first slice came from the bottom of these samples, leading to more reliable results. Care must be taken to ensure the sectioning is appropriately labelled and handled to avoid any missteps. When using the method on a novel sheet, section from both orientations initially to determine which is more suitable.

Another potential improvement is calibrating the nitrogen concentration to the actual chemical concentration. The results shown in this paper are nitrogen concentrations (nitrogen counts/mg), but this can be easily combined with retention analysis at a known dose to determine an actual chemical concentration at any point in the sheet.

ABOUT THIS PAPER

Cite this article as:
Nicholas, M., Bliss, T., and Bohnsack, T., *TAPPI J.* 22(1): 40(2023). https://doi.org/10.32964/TJ22.1.40

DOI: https://doi.org/10.32964/TJ22.1.40

ISSN: 0734-1415

Publisher: TAPPI Press

Copyright: ©TAPPI Press 2023

About this journal

CONCLUSIONS

The fluorescent staining and CLSM method offers a quick and reliable way to visually check the chemical distribution when an appropriate sheet is used. This method is more suitable for laboratory-produced handsheets, but the technique can be used to help refine understanding of the foam application process and how its variables can affect the chemical distribution.

The layer sectioning and nitrogen analysis method can generate a plot of added DSA concentration through the z-direction of the sheet. This method should be useful in a range of applications, including commercially generated paper products. Chemical distribution results can give additional meaning to strength tests and help us to improve and understand the foam-assisted additive addition process. This method visualizes the chemical distribution after subtracting any interference from the base sheet, and it can provide meaningful differentiation between similar treatment conditions. Although the method has some limitations, it should be broadly applicable to a variety of potential additives and substrates, provided the additives contain detectable amounts of nitrogen. **TJ**

ACKNOWLEDGMENTS

The authors wish to acknowledge the many individuals who contributed to the development of the techniques herein described and to Solenis management for permitting publication. Special thanks to Jean Ross at the University of Delaware, Bioimaging Center for cryostat sectioning, which is supported by grant NIH-NIGMS (P20 GM103446). The CLSM equipment was acquired with a shared instrumentation grant (S100D016361) and access was supported by the NIH-NIGMS (P20 GM103446), the NSF (IIA-1301765), and the State of Delaware.

ABOUT THE AUTHORS

We studied this topic because we had a commercial need for a method of z-direction analysis in order to qualify the characteristics of foam-applied chemistry. This study complements a lot of recent research into foam application onto the wet web before pressing.The most difficult aspect of this study was finding a method of sectioning the sheet. We researched a variety of methods that are mentioned in the paper, but using a cryogenic microtome to cut parallel to the sheet surface was a unique and useful solution.

Through this work, we found a novel method for testing and quantifying the z-direction chemical distribution in a foam-treated sheet. The most interesting finding was that there was incomplete penetration of the substrate, as the back side of the sheet did not contain any foam-added chemistry.

For mills, there is the potential for targeted application of chemistry in certain problem areas.



Nicholas



Bliss



Bohnsack

Our next step is utilizing this method to better understand the variables that affect chemical distribution after foam application.

Nicholas is process research engineer, Bliss is research Fellow, and Bohnsack is analytical chemist at Solenis LLC in Wilmington, DE, USA. Email Nicholas at mnicholas@solenis.com.

LITERATURE CITED

1. Tanaka, H., Luner P., and Cote, W., *Tappi* 65(4): 95(1982).
2. Attwood, B.W. and Loy, K.W.H., *Tappi J.* 76(10): 160(1993).
3. Marton, J. and Marton, T., *Tappi* 59(12): 121(1976).
4. Price, C. and Hubbe, M.A., *TAPPI J.* 20(1): 21(2021). https://doi.org/10.32964/TJ20.1.21.
5. Foulger, M., Parisian, J., Didwania, H.P., et al., *Pulp Pap. Can.* 100(2): 24(1999).
6. Krause, A., Rieck, J., Lucas, D., et.al., U.S. pat. application 2019/0368122 A1 (Dec. 5, 2019).
7. Bliss, T., Luo, M., and Nicholas, M., *TAPPI J.* 20(1): 9(2021). https://doi.org/10.32964/TJ20.1.9.
8. Kinnunen-Raudaskoski, K., Saliminen, K., Lehmonen, J., et.al., *TAPPI J.* 15(11): 731(2016). https://doi.org/10.32964/TJ15.11.731.
9. Bando, T., Sakamoto, K., and Iwata, H., *Jpn. TAPPI J.* 49(5): 841(1995). https://doi.org/10.2524/jtappij.49.841.
10. Erikka, A., Pakarinen, P., and Odell, M., *Pulp Pap. Can.* 99(1): 81(1998).
11. Puurtinen, A., *Pap. Technol.* 44(4): 33(2003).
12. Pritchard, E.J., *Br. Pap. Board Makers' Assoc., Proc. Tech. Sect.* 38(2): 426(1951).
13. Anon., "Sheet splitting laboratory brochure," FPInnovations, Pointe Claire, QC, Canada (undated; received May 2008).
14. Modgi, S., McQuaid, M.E., and Englezos, P., *Nord. Pulp Pap. Res. J.* 21(5): 659(2006). https://doi.org/10.3183/npprj-2006-21-05-p659-664.
15. Parker, J. and Mih, W.C., *Tappi* 47(5): 254(1964).
16. Hansen, E., *Tappi* 34(4): 180(1951).
17. Browning, B.L. and Isenberg, I.H., *Tappi* 38(10): 602(1955).
18. Lipponen, J., Lappalainen, T., Astola, J., et al., *Nord. Pulp Pap. Res. J.* 19(3): 300(2004). https://doi.org/10.3183/npprj-2004-19-03-p300-308.
19. Ozaki, Y., Bousfield, D.W., and Shaler, S.M., *Appita J.* 59(4): 326(2006).
20. Wilhelm, S., Grobler, B., Gluch, M., et al., *Confocal Laser Microscopy: Principles*, Carl Zeiss, 2003.